LASER INTERFEROMETER GRAVITATIONAL WAVE OBSERVATORY

LIGO Laboratory / LIGO Scientific Collaboration

LIGO-T0900103-v2draft *ADVANCED LIGO* 11 Mar 2009

Hysteresis and pitch mode Q in the quad noise prototype and possible implications for thermal noise

Mark Barton

Distribution of this document:
DCC

This is an internal working note
of the LIGO Project.

California Institute of Technology
LIGO Project – MS 18-34
1200 E. California Blvd.
Pasadena, CA 91125
Phone (626) 395-2129
Fax (626) 304-9834
E-mail: info@ligo.caltech.edu

Massachusetts Institute of Technology
LIGO Project – NW22-295
185 Albany St
Cambridge, MA 02139
Phone (617) 253-4824
Fax (617) 253-7014
E-mail: info@ligo.mit.edu

LIGO Hanford Observatory
P.O. Box 1970
Mail Stop S9-02
Richland WA 99352
Phone 509-372-8106
Fax 509-372-8137

LIGO Livingston Observatory
P.O. Box 940
Livingston, LA 70754
Phone 225-686-3100
Fax 225-686-7189

http://www.ligo.caltech.edu/

Table of Contents

1 Introduction

1.1 Purpose and Scope

In suspending and debugging the quad test mass suspension noise prototype at LASTI, Brett Shapiro discovered a significant amount of hysteresis in the pitch degree of freedom. This document describes some analysis that was done using the Mathematica quad suspension model by Mark Barton to try to match the measured mode Qs and thus find clues as to which element or elements in the suspension were hysteretic.

1.2 References

Pitch Tests on the LASTI Quad Noise Prototype (T080040-00)

TILT TESTS ON RAL NOISE PROTOTYPE (T080030-00)

Tests with single two-wire pendulum (T080033-00)

QUAD SUS: Summary of observations on anomalous tilts (T080036-00)

QUAD SUS: bending stresses in wires as masses are tilted (T080037-00)

Dissipation processes in Metal springs, Ascione et al. (G080574-00)

Studies of Hysteresis in metals, DeSalvo et al. (G080243-00)

Dislocation movement and hysteresis in Maraging blades, Di Cintio et al. (P0900028-v1)

Thermal noise in mechanical experiments, P. Saulson, Phys. Rev. D, 42:2437 (1990)

On a Theorem of Irreversible Thermodynamics, H.B. Callen and R.F. Greene, Phys. Rev., 86:702-10 (1952)

1.3 Version history

11/8/08: First draft.

3/4/09: Second draft with final numbers and provisional conclusions.

3/10/09: v1 with Norna's feedback, appendices with parameters.

3/11/09: v2 draft with bottom wire data, better diagram, more on Justin and Riccardo's results.

3/12/09: v2.

2 The problem

When the quad noise prototype was suspended at LASTI, significant pitch hysteresis was noted. When a large pitch displacement was applied at the top or upper intermediate masses, the pendulum would take a significant set in pitch, of order 5% of the applied displacement.

This hysteresis is a potential problem in two ways. First, it is a practical issue for aligning the pendulum in pitch, because the pitch angle is not a simple function of the position of the trim mass but depends on the past history of the pendulum in a non-obvious way. Second, the magnitude of the effect is so gross that if it generates thermal noise as for other sorts of damping, then even if it

is confined to the top levels of a build with a monolithic stage, one might reasonably worry that it would bypass the filtering effect of the lower stages and result in excess noise at the optic.

A major program of investigation was undertaken on both the LASTI and RAL noise prototype builds and on a test pendulum at RAL, resulting in reports by Brett Shapiro (T080040-00) and Justin Greenhalgh et al. (T080030-00, T080033-00, T080036-00, T080037-00). It was established that some of the initial misbehaviour at LASTI was probably due to loose blade clamps (especially one that had been improperly reworked) but when it was corrected, only about half the effect went away. Also, tests at RAL on a pendulum without blades still showed an effect. DeSalvo et al. have suggested that there may be a hysteretic effect in the wire material analogous to that seen in the SAS blades (G080243-00, G080574-00, P0900028-v1) but misbehaviour in the wire clamps has not been ruled out.

One data set that has not been fully analyzed before now is the pitch transfer functions made for the LASTI quad in vacuum by Brett Shapiro. The Q's of the first three pitch modes were determined from the plot of the transfer function of pitch actuation at the top mass to pitch of the top mass. See Figure 1. (The peaks for the fourth and highest pitch mode and for the coupled longitudinal modes could in principle supply additional information, but unfortunately these were too narrow to resolve with the measurement duration that could be allocated at the time.)

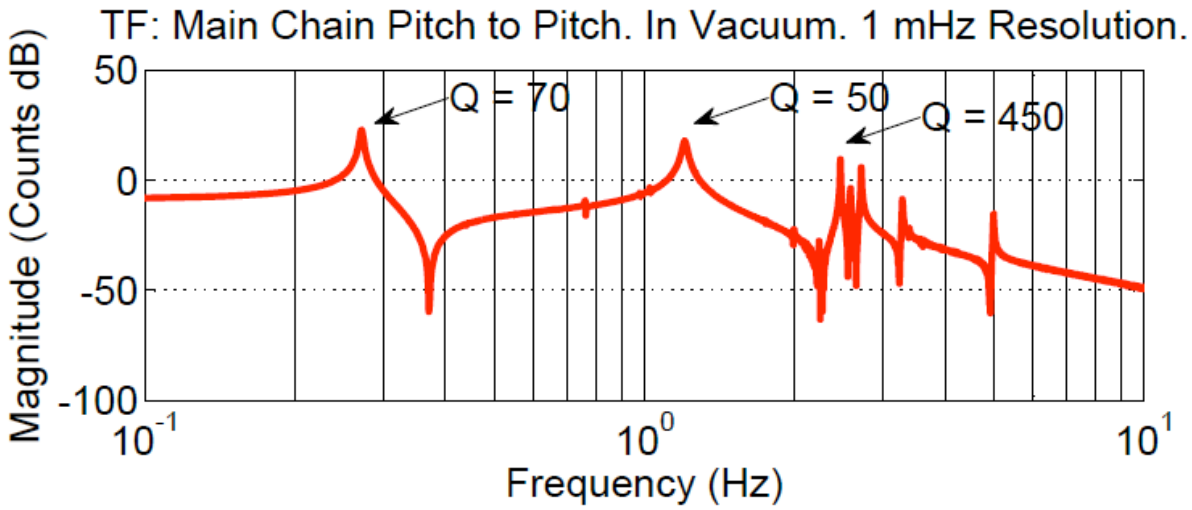

Figure 1: Top mass pitch-pitch transfer function of LASTI quad main chain from Brett Shapiro

These Q's presumably imply something about the location of the damping, but interpreting them is tricky, partly because of the complexity of the system and partly because the exact nature of the loss is unknown. To get some insight, loss was applied at different points in a Mathematica model of the suspension as described in the next section to see if the values could be reproduced.

3 Modeling

3.1 Model and parameter set

To see whether the observed Q's could be accounted for, a custom version of the Mathematica Quad Lateral model was prepared. The standard Quad Lateral model (see T020205-02)

incorporates all the physics we have previously found to be required and sufficient to account for the mode structure of the pendulum:

- Four rigid bodies, each with off-diagonal as well as diagonal components of MOI
- Six blade springs, each with both vertical and lateral (that is, with respect to the blade, or longitudinal with respect to the pendulum) compliance
- 14 wires, each with longitudinal and bending elasticities.

The parameter set used was one developed by Brett Shapiro (see Section 6), which is mostly based on measured numbers for the as-built system but with tweaks to accurately reproduce the measured main chain mode frequencies. The standard version of the model allows for a different loss function on each different component of elasticity except that the loss function of the blades is the same in both vertical and lateral. Because the difference between vertical and lateral loss was suspected to be important, the structure of the model was adjusted to separate these. Conversely, since blade vertical was suspected to be irrelevant, a single run was done with extra vertical damping in all blades. The model was run multiple times with large amounts of additional damping injected at different locations in turn. (The default damping sources, from Bench/GWINC, were left enabled because they were negligible in comparison.)

3.2 Details of additional damping

For the first round of simulations, the additional damping was taken to be structural with phi(f) = 0.05. The value of 0.05 was chosen to be numerically equal to a typical fractional pitch offset induced in the pendulum by a pitch excursion. That is not to suggest that the hysteresis is thought to be identical to structural damping – structural damping is merely the most similar phenomenon that can be implemented with a linear model. The key difference is that observed hysteresis apparently contains a significant component of static friction, because a semi-permanent set can be induced by a large but brief excursion. By contrast, structural damping is effectively implemented by the spring-dashpot model shown in Figure 2 (see Saulson 1990) and cannot reproduce that behaviour. The primary spring represents the stiffness at DC, and the secondary spring-dashpot units have time constants that vary over a wide frequency range so as to give a constant loss angle. This implies that during a pulse excitation, the longer time-constant dashpots will not have time to move, so that the relaxation to the initial condition afterwards will be of the same time-scale as the pulse.

The reason that structural damping may be relevant despite these caveats is that it is very likely a worst case. According to the Fluctuation Dissipation Theorem (Callen 1952), thermal noise is associated with energy loss for microscopic amplitudes. Structural damping will dissipate approximately as much energy as friction for large amplitudes, but a frictional effect is likely to have some degree of lock-up for smaller motions and one might hope that this would result in less thermal noise.

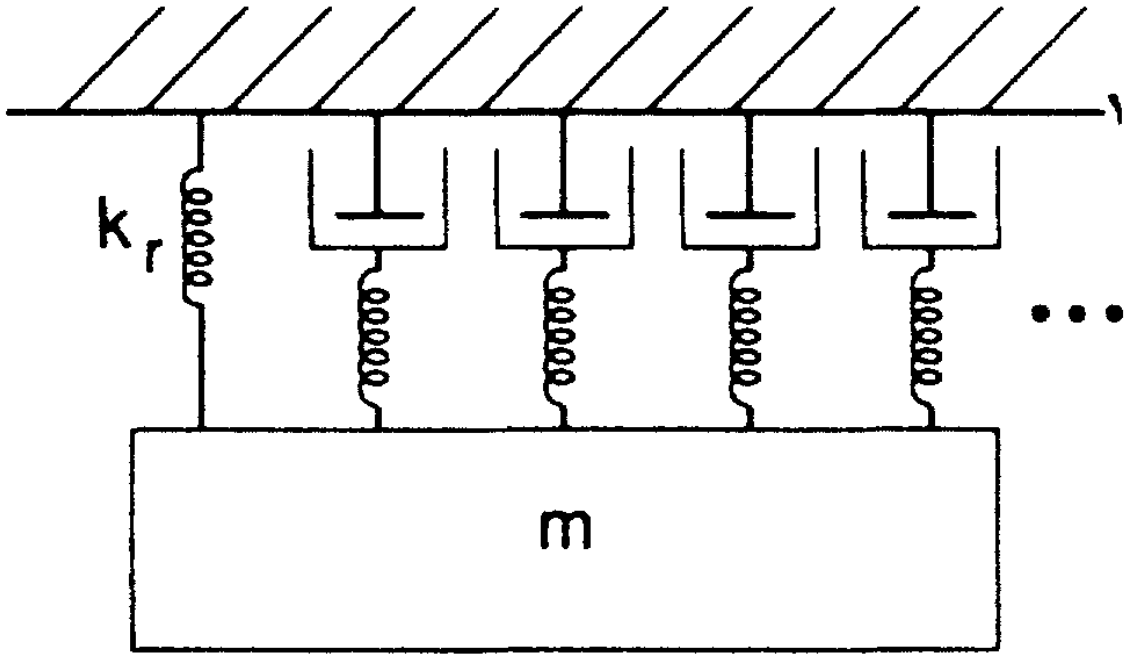

Figure 2: Conceptual model of a spring with arbitrary frequency-dependent damping (from Saulson 1990)

3.3 First round results

To begin with, damping was applied according to the scheme in Figure 3/ Table 1.

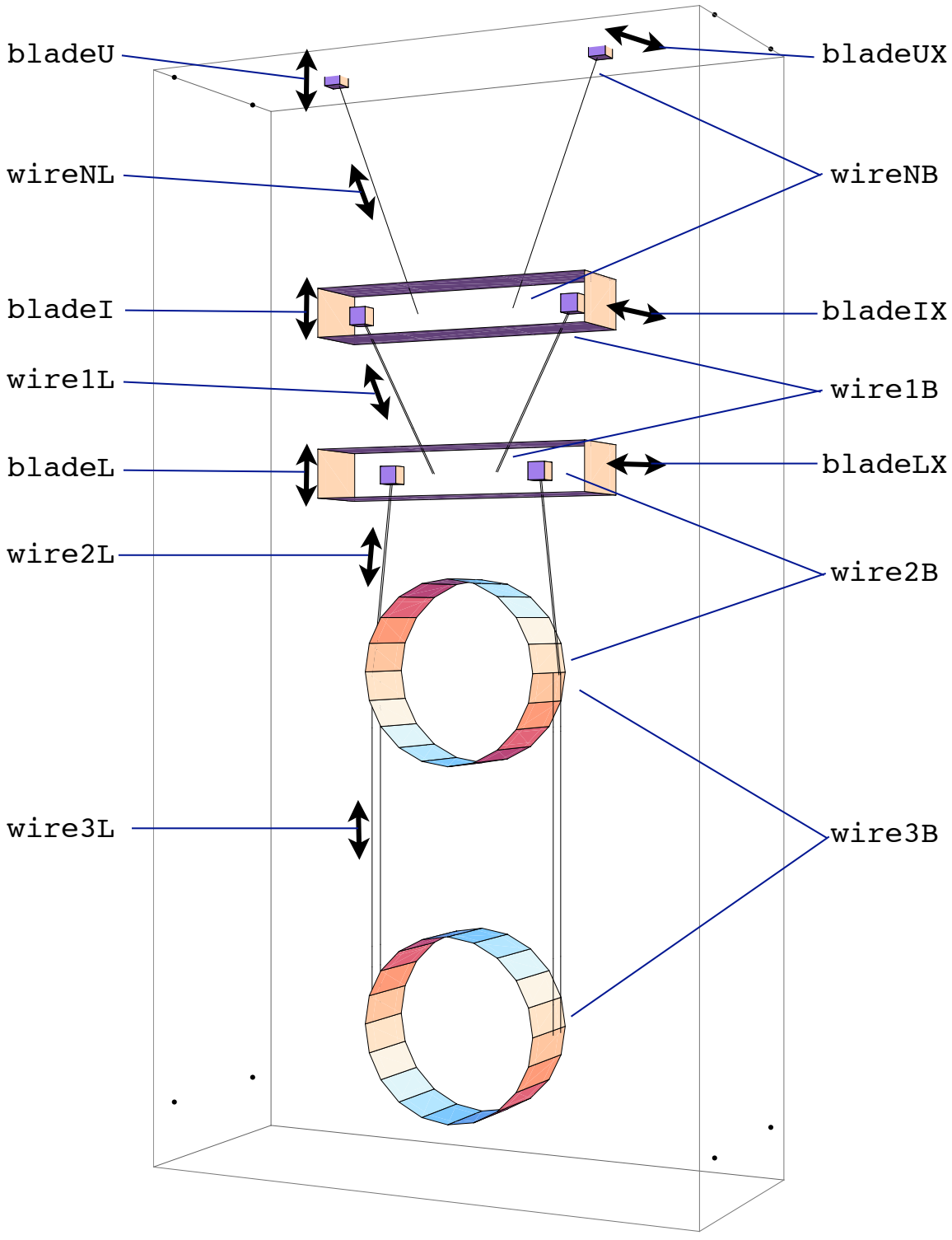

Figure 3: Key to damping location tags

Damping location	Identifying tag	Value
No extra damping	`orig`	0
All blades vertical	`bladeV`	0.05 each
Top blade lateral	`bladeUX`	0.05
Top wire bending	`wireNB`	0.05
Top wire longitudinal	`wireNL`	0.05
Intermediate blade lateral	`bladeIX`	0.05
Second-top wire bending	`wire1B`	0.05
Second-top wire longitudinal	`wire1L`	0.05
Bottom blade lateral	`bladeLX`	0.05
Second bottom wire bending	`wire2B`	0.05
Second bottom wire longitudinal	`wire2L`	0.05
Bottom wire bending	`wire3B`	0.05
Bottom wire longitudinal	`wire3L`	0.05

Table 1: types and amounts of damping in Round 1.

The resulting Q values were extracted from the calculated transfer function from pitch of the top mass to pitch of the top mass using an semi-automatic Q-finding routine that searched numerically for the peak and half-power points. The results are shown in Table 1. Loss in the blade vertical DOFs (`bladeV`) or the top blade lateral DOF (`bladeUX`) did not drag down the Qs significantly relative to the original condition (`orig`) and so these locations are exonerated.

```
          Q1       Q2       Q3       Q4
orig     1387.75  2263.89  5056.12  5439.99
bladeV   1387.26  2257.29  4946.66  2990.02
bladeUX  1387.5   2258.83  5055.65  5439.98
wireNB   51.2254  55.2475  818.441  1413.96
wireNL   52.3179  56.4505  833.604  1437.83
bladeIX  29.0315  31.1175  476.15   702.98
wire1B   43.8728  79.512   644.845  677.725
wire1L   42.8095  51.3195  33.5011  27.2258
bladeLX  27.871   102.078  268.348  267.108
wire2B   33.2823  307.035  961.672  836.504
wire2L   27.6608  41.1012  400.458  30.4395
wire3B   67.7243  1938.93  3398.68  4063.99
wire3L   66.2595  574.921  4.26949  28.6169
```

Table 2: Q values in Round 1. These are to be compared with measured values Q1=70, Q2=50, Q3=450 and Q4=large.

To make comparisons with the observed values easier, each row was scaled to make Q1=70, assuming linearity.

	Q1	Q2	Q3	Q4
orig	70.	114.193	255.037	274.399
bladeV	70.	113.901	249.605	150.874
bladeUX	70.	113.959	255.059	274.449
wireNB	70.	75.4963	1118.41	1932.2
wireNL	70.	75.5293	1115.34	1923.78
bladeIX	70.	75.0298	1148.08	1695.01
wire1B	70.	126.863	1028.86	1081.33
wire1L	70.	83.9152	54.7794	44.5184
bladeLX	70.	256.376	673.977	670.861
wire2B	70.	645.76	2022.6	1759.35
wire2L	70.	104.013	1013.42	77.032
wire3B	70.	2004.08	3512.88	4200.55
wire3L	70.	607.376	4.51051	30.2324

Table 3: Q values from Round 1, with each row scaled to Q1=70. These are to be compared with measured values Q1=70, Q2=50, Q3=450 and Q4=large.

3.4 Second round results

Then, as a check on the assumption of linearity, the same scale factors (Q1/70, for Q1 in Table 1) were applied to the values of phi (all originally 0.05), and selected rows of Table 1 were recomputed, giving Table 4 (in Section 0). The values are similar to Table 3 at the 10-20% level, confirming approximate linearity. (Perfect linearity is not to be expected because the Bench/GWINC damping was left unscaled.)

	phi	Q1	Q2	Q3	Q4
wireNBlincheck	0.0365895	69.1471	74.8281	1055.69	1764.57
wireNLlincheck	0.0373699	69.1936	74.8991	1056.4	1766.41
bladeIXlincheck	0.0207368	67.9774	73.3409	1011.46	1436.39
wire1Blincheck	0.0313377	68.8874	124.267	956.022	1008.66
wire1Llincheck	0.0305782	68.8559	82.6695	99.4754	98.6574
bladeLXlincheck	0.0199078	68.2316	239.361	593.743	630.95
wire2Blincheck	0.0237731	68.6395	561.714	1671.64	1506.45
wire2Llincheck	0.0197577	68.6076	101.145	901.213	215.41
wire3Blincheck	0.0483745	69.8944	1948.02	3435.28	4097.69
wire3Llincheck	0.0473282	69.8262	598.624	4.23106	58.6316

Table 4: Q values from Round 2, using a different scaling method from Table 3. Again, these are to be compared with measured values Q1=70, Q2=50, Q3=450 and Q4=large.

3.5 Comparison with measured Qs

None of the rows of Table 4 was a perfect match to the observed signature. wireNB, wireNL and bladeIX were closest, with the only discrepancy was that Q2 was slightly bigger than Q1, instead of slightly less (50/70). However several more damping locations can be more confidently excluded:

- Not `wire2L` or `wire3L` because Q4 too low.
- Not `wire3B` because Q2 too high.
- Not `wire2B` because Q3 too high.
- Not `bladeLX` because Q2 too high.
- Not `wire1L` because Q3, Q4 too low.
- Possibly `wire1B` but Q2 rather high.
- Possibly `wireNB`, `wireNL` or `bladeIX` but Q2 a bit high.

The fact that wireNB and wireNL give similar Q values in fact says that it is the bending loss of the wire rather than the longitudinal stretching that is important. This is because the Mathematica model uses the longitudinal loss factor for the extra extension due to the bending of the wire away from the straight line between the endpoints and the energy associated with this is the same as for the pure bending energy. (By contrast, wire2L has a much larger effect on Q4 than wire2B reflecting that longitudinal stretch is important in that mode. See the mode shapes in .) The Mathematica model does not directly include slippage of wires at the clamp but the bending component of the wire loss is likely to be a good proxy (unfortunately so from the point of view of telling them apart).

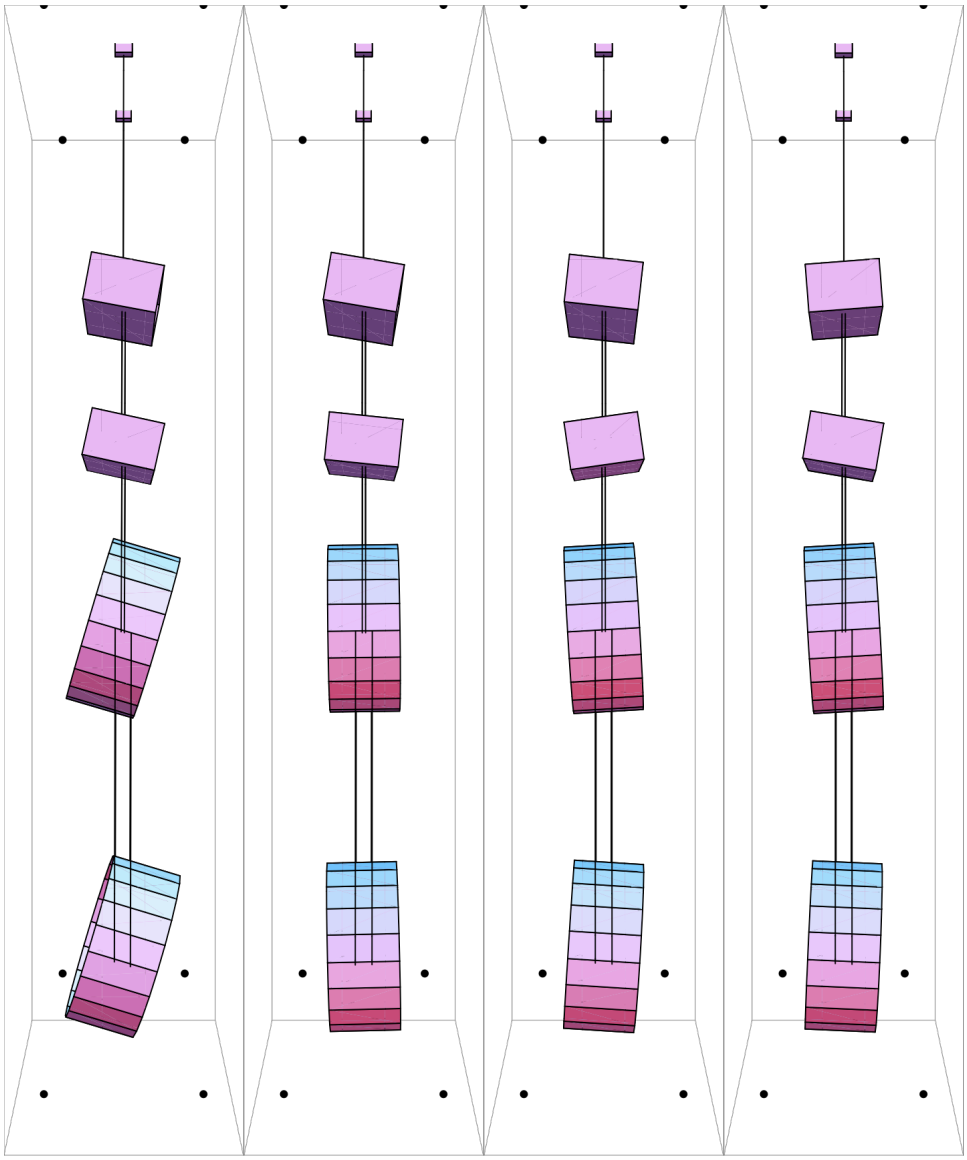

Figure 4: Mode shapes for the pitch modes (1, 9, 15, 17) of the all-metal build.

4 Application to prospective build with monolithic stage

To check the implications for the final system, a model was prepared with the upper stages per Brett Shapiro's parameter set and a monolithic lower stage per T080091-00 and M080134-00. The Qs are given in Table 5, and the resulting thermal noise is given in Figure 5.

	phi	Q1	Q2	Q3	Q4
wireNBmatch	0.0365895	128.354	9230.91	298.219	677.955
wireNLmatch	0.0373699	125.696	9034.88	292.142	665.325
bladeIXmatch	0.0207368	243.771	56 241.2	545.599	967.332
wire1Bmatch	0.0313377	135.955	25 066.2	230.736	83.2569
wire1Lmatch	0.0305782	139.298	25 657.	236.362	28.3243
bladeLXmatch	0.0199078	275.512	72 880.8	6392.01	278.404
wire2Bmatch	0.0237731	158.145	14 187.6	246.489	162.747
wire2Lmatch	0.0197577	189.633	17 016.7	295.44	196.152

Table 5: Qs for a hypothetical pendulum with the same upper stages as previously, the same damping factors as Table 4, but a monolithic lower stage per T080091-00 and M080134-00.

5 Conclusion

If the misbehaviour is at a low level in the chain, and especially in the wires holding the penultimate mass, then there could be excess thermal noise at the mass. However if the misbehaviour is mostly in the upper wires (or wire clamps) and/or the middle blades as seems to be indicated by the results of Section 3.5, then the thermal noise will be much higher than previously calculated at low frequencies but should asymptote away by the start of the measurement band at 10 Hz.

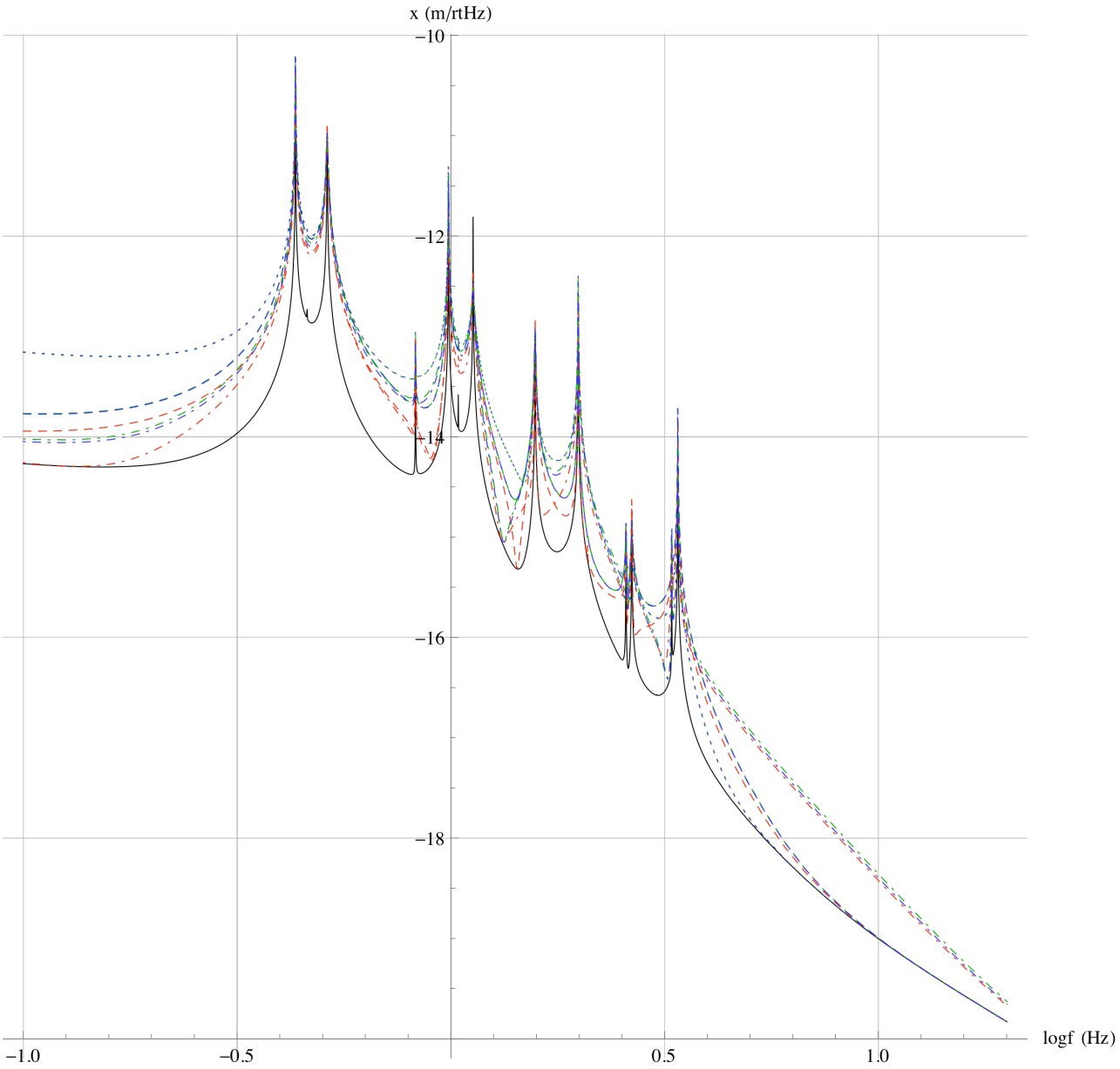

blade lateral: red; intermediate: dashed; lower dot-dashed.
wire bending: green; N: dotted; 1: dashed; 2: dot-dashed.
wire longitudinal: blue; N: dotted; 1: dashed; 2: dot-dashed.

Figure 5: Thermal noise for monolithic stage and damping per Table 4.

6 Appendix

6.1 Parameter set used for all-metal build

```
overrides = {
      ribbons -> False,
      nx -> 0.1300, (* T040214-01 *)
      ny -> 0.5000, (* T040214-01 *)
      nz -> 0.0840, (* T040214-01 *)
```

```
denn -> 4000, (* T040214-01 *)
mn -> 21.924, (* BNS - measured 11/21/07 *)
Inx -> 0.461468580178307, (* Model Fit: gradient_descent_fit_roll.m; BNS
      7/30/08 *)
Iny -> 0.079141440690845, (* Model Fit: gradient_descent_fit_pitch.m; BNS
      7/30/08 *)
Inz -> 0.46233, (* Model Fit: gradient_descent_fit_yaw.m; BNS 7/29/08 *)
Inxy -> -0.033612681822167, (* Model Fit: gradient_descent_fit_roll.m;
      BNS 7/30/2008 *)
Inyz -> 0.0000439, (* ? *)
Inzx -> 0.00198, (* ? *)
Inxz -> Inzx,
Inzy -> Inyz,
Inyx -> Inxy,
ux -> 0.1300, (* T040214-01 *)
uy -> 0.5000, (* T040214-01 *)
uz -> 0.0840, (* T040214-01 *)
den1 -> 4000, (* T040214-01 *)
m1 -> 22.005, (* BNS - measured 11/21/07 *)
I1x -> 0.540861597136711, (* Model Fit: gradient_descent_fit_roll.m; BNS
      7/30/08 *)
I1y -> 0.077486282188856, (* Model Fit: gradient_descent_fit_pitch.m; BNS
      7/30/08 *)
I1z -> 0.51758, (* Model Fit: gradient_descent_fit_yaw.m; BNS 7/29/08 *)
I1xy -> -0.026034877679599, (* Model Fit: gradient_descent_fit_roll.m;
      BNS 7/30/08 *)
I1yz -> 0, (* ? *)
I1zx -> 0, (* ? *)
I1xz -> I1zx,
I1zy -> I1yz,
I1yx -> I1xy,
ix -> 0.1300, (* T040214-01 *)
ir -> 0.1570, (* T040214-01 *)
den2 -> 2200, (* not used *)
m2 -> 39.664, (* measured, BNS -  measured 11/21/07 *)
I2x -> 0.614736940669984, (* Model Fit: gradient_descent_fit_roll.m; BNS
      7/30/08 *)
I2y -> 0.407761183645900, (* Model Fit: gradient_descent_fit_pitch.m; BNS
      7/30/2008 *)
I2z -> 0.41557, (* Model Fit: gradient_descent_fit_yaw.m; BNS 7/29/08 *)
tx -> 0.1300, (* T040214-01 *)
tr -> 0.1570, (* T040214-01 *)
den3 -> 2200, (* not used *)
m3 -> 39.558, (* BNS -  measured 11/21/07 *)
I3x -> 0.614281054577945, (* Model Fit: gradient_descent_fit_roll.m; BNS
      7/30/08 *)
I3y -> 0.413139474164149, (* Model Fit: gradient_descent_fit_pitch.m; BNS
      7/30/08 *)
I3z -> 0.40046, (* Model Fit: gradient_descent_fit_yaw.m; BNS 7/29/2008
      *)
ln -> 0.448574, (* ? *)
l1 -> 0.308993, (* ? *)
l2 -> 0.341653, (* ? *)
l3 -> 0.600648, (* ? *)
rn -> (1.1/2)*10^-3, (* "Useful data for Noise Prototype Quad assembly";
      BNS 6/18/08 *)
r1 -> (0.71/2)*10^-3, (* "Useful data for Noise Prototype Quad assembly";
      BNS 6/18/08 *)
```

```
r2 -> (0.635/2)*10^-3, (* "Useful data for Noise Prototype Quad
      assembly"; BNS 6/18/08 *)
r3 -> (0.457/2)*10^-3, (* "Useful data for Noise Prototype Quad
      assembly"; BNS 6/18/08 *)
Yn -> 2.12000 10^+11, (* "As Designed Parameter Set 2"; BNS 6/18/08 *)
Y1 -> 2.12000 10^+11, (* "As Designed Parameter Set 2"; BNS 6/18/08 *)
Y2 -> 2.12000 10^+11, (* "As Designed Parameter Set 2"; BNS 6/18/08 *)
Y3 -> 2.12000 10^+11, (* "As Designed Parameter Set 2"; BNS 6/18/08 *)
kbuz -> 1411.464026291042094835154548O224, (* See matlab code
      spring_stiffness_calc: BNS 6/19/08 *)
kbiz -> 1650.524059045379672879214321792, (* See matlab code
      spring_stiffness_calc: BNS 6/19/08 *)
kblz -> 2423.519015280238231051986O608100, (* See matlab code
      spring_stiffness_calc: BNS 6/19/08 *)
dm -> -0.003320022822893, (* Model Fit d's: gradient_descent_fit_pitch.m
      and gradient_descent_fit_roll.m; BNS 7/30/2008 *)
dn -> 0.002252503151706, (* Model Fit d's: gradient_descent_fit_pitch.m
      and gradient_descent_fit_roll.m; BNS 7/30/2008 *)
d0 -> -0.001663908530073, (* Model Fit d's: gradient_descent_fit_pitch.m
      and gradient_descent_fit_roll.m; BNS 7/30/2008 *)
d1 -> 0.002364277173936, (* Model Fit d's: gradient_descent_fit_pitch.m
      and gradient_descent_fit_roll.m; BNS 7/30/2008 *)
d2 -> -0.002987230839186, (* Model Fit d's: gradient_descent_fit_pitch.m
      and gradient_descent_fit_roll.m; BNS 7/30/2008 *)
d3 -> -0.000101947264237, (* Model Fit d's: gradient_descent_fit_pitch.m
      and gradient_descent_fit_roll.m; BNS 7/30/2008 *)
d4 -> -0.002363109092631, (* Model Fit d's: gradient_descent_fit_pitch.m
      and gradient_descent_fit_roll.m; BNS 7/30/2008 *)
sn -> 0,    (* T040214-01 *)
su -> 0.003,  (* T040214-01 *)
si -> 0.003,  (* T040214-01 *)
sl -> 0.015,  (* T040214-01 *)
nn0 -> 0.250,  (* T040214-01 *)
nn1 -> 0.090,  (* T040214-01 *)
n0 -> 0.200,  (* T040214-01 *)
n1 -> 0.060,  (* T040214-01 *)
n2 -> 0.140,  (* T040214-01 *)
n3 -> 0.1762, (* "As Designed Parameter Set 2"; BNS 6/18/08 *)
n4 -> 0.1712, (* "As Designed Parameter Set 2"; BNS 6/18/08 *)
n5 -> 0.1712, (* "As Designed Parameter Set 2"; BNS 6/18/08 *)
nwn -> 2,
nw1 -> 4,
nw2 -> 4,
nw3 -> 4,
mn3 -> mn+m13,
m13 -> m1+m23,
m23 -> m2+m3,
kbux -> 1.0 10^5,  (* as for middle *)
kbix -> 1.0 10^5,  (* Justin 11/29/05 *)
kblx -> 0.8 10^5,  (* Ian 12/09/05 *)
flexn -> Sqrt[nwn Mn1 Yn/(mn+m1+m2+m3)/g]*cn^(3/2),
flex1 -> Sqrt[nw1 M11 Y1/(m1+m2+m3)/g]*c1^(3/2),
flex2 -> Sqrt[nw2 M21 Y2/(m2+m3)/g]*c2^(3/2),
flex3 -> Sqrt[nw3 M31 Y3/m3/g]*c3^(3/2),
thetan -> 180 ArcSin[sin]/Pi,
theta1 -> 180 ArcSin[si1]/Pi,
theta2 -> 180 ArcSin[si2]/Pi,
theta3 -> 180 ArcSin[si3]/Pi,
```

```
      rhosilica -> 2.2 10^3, (* IFOModel v4.1 *)
      Csilica -> 770., (* AH silica spec sheet, summary email by MB, 3/13/08 *)
      Ksilica -> 1.38,  (* IFOModel v4.1 *)
      sigmasilica -> 0.17,
      Gsilica -> Ysilica/2/(1+sigmasilica), (* shear modulus *)
      alphasilica -> 3.9 10^-7, (* AH measurement, summary email by MB, 3/13/08
            *)
   betasilica -> 1.52 10^-4, (* IFOModel v4.1 *)
    phisilica -> 4.1 10^-10, (* IFOModel v4.1 *)
   phissilica -> 3. 10^-11, (* surface *)
      Ysilica -> 7.2 10^10, (* AH spec sheet, summary email by MB, 3/13/08 *)
      dssilica -> 1.5 10^-2, (* IFOModel v4.1 *)
      sigmasilica -> 0.17,
      Gsilica -> Ysilica/2/(1+sigmasilica), (* shear modulus *)

      rhosteel -> 7800., (* gwinc/IFOModel v1.0 *)
      Csteel -> 486., (* gwinc/IFOModel v1.0 *)
      Ksteel -> 49., (* gwinc/IFOModel v1.0 *)
      alphasteel -> 12. 10^-6, (* gwinc/IFOModel v1.0 *)
            betasteel -> -2.5 10^-4, (* gwinc/IFOModel v1.0 *)
      phisteel -> 2. 10^-4, (* gwinc/IFOModel v1.0 = Geppo's value  *)
      Ysteel -> 2.12 10^+11, (* measured by MB, 11/18/05 *)

      rhomarag -> 7800., (* gwinc/IFOModel v1.0 *)
      Cmarag -> 460., (* gwinc/IFOModel v1.0 *)
      Kmarag -> 20., (* gwinc/IFOModel v1.0 *)
      alphamarag -> 11. 10^-6, (* gwinc/IFOModel v1.0 *)
      betamarag -> -2.5 10^-4, (* Geppo's value - gwinc/IFOModel v1.0 is wrong
            *)
      phimarag -> 1. 10^-4, (* gwinc/IFOModel v1.0 *)
      Ymarag -> 1.87 10^11, (* gwinc/IFOModel v1.0 *)

(* Zener, 1938, Phys. Rev. 53:90-99 *)
      magicnumber®1/4/FindRoot[0==D[BesselJ[1,x],x],{x,1.8}][[1,2]]^2,

      tmU -> 0.0043, (* IFOModel v4.1 *)
      deltabladeU ® Ymarag*alphamarag^2*temperature/(rhomarag*Cmarag),
      taubladeU ® rhomarag*Cmarag*tmU^2/(Kmarag*N[Pi]^2),
      damping[imag,bladeUtype] ® ((phimarag+
deltabladeU*(2*N[Pi]*#1*taubladeU)/(1+(2*N[Pi]*#1*taubladeU)^2))&),

      tmI -> 0.0046, (* IFOModel v4.1 *)
deltabladeI ® Ymarag*alphamarag^2*temperature/(rhomarag*Cmarag),
      taubladeI ® rhomarag*Cmarag*tmI^2/(Kmarag*N[Pi]^2),
      damping[imag,bladeItype] ® ((phimarag+deltabladeI*(2*N[Pi]*#1*taubladeI)
      /(1+(2*N[Pi]*#1*taubladeI)^2))&),

      tmL -> 0.0042, (* IFOModel v4.1 *)
deltabladeL ® Ymarag*alphamarag^2*temperature/(rhomarag*Cmarag),
      taubladeL ® rhomarag*Cmarag*tmL^2/(Kmarag*N[Pi]^2),
      damping[imag,bladeLtype] ® ((phimarag+deltabladeL*(2*N[Pi]*#1*taubladeL)
      /(1+(2*N[Pi]*#1*taubladeL)^2))&),

deltawireU ® Ysteel*temperature
      *(alphasteel-betasteel*g*(mn+m1+m2+m3)/(nwn*N[Pi]*rn^2*Ysteel))^2
```

```
  /(rhosteel*Csteel),
      tauwireU ® magicnumber*rhosteel*Csteel*(2*rn)^2/Ksteel,
      damping[imag,wireUtype] ® (phisteel&),
      damping[imag,wireUatype] ® ((phisteel+deltawireU*(2*N[Pi]*#1*tauwireU)
      /(1+(2*N[Pi]*#1*tauwireU)^2))&),

      deltawireI ® Ysteel*temperature
      *(alphasteel-betasteel*g*(m1+m2+m3)/(nw1*N[Pi]*r1^2*Ysteel))^2
      /(rhosteel*Csteel),
 tauwireI ® magicnumber*rhosteel*Csteel*(2*r1)^2/Ksteel,
      damping[imag,wireItype] ® (phisteel&),
      damping[imag,wireIatype] ® ((phisteel+deltawireI*(2*N[Pi]*#1*tauwireI)
      /(1+(2*N[Pi]*#1*tauwireI)^2))&),

      deltawireL ® Ysteel*temperature
      *(alphasteel-betasteel*g*(m2+m3)/(nw2*N[Pi]*r2^2*Ysteel))^2
      /(rhosteel*Csteel),
 tauwireL ® magicnumber*rhosteel*Csteel*(2*r2)^2/Ksteel,
      damping[imag,wireLtype] ® (phisteel&),
      damping[imag,wireLatype] ® ((phisteel+deltawireL*(2*N[Pi]*#1*tauwireL)
      /(1+(2*N[Pi]*#1*tauwireL)^2))&),

      deltafibre ® Ysteel*temperature
      *(alphasteel-betasteel*g*m3/(nw3*N[Pi]*r3^2*Ysteel))^2
      /(rhosteel*Csteel),
 taufibre ® magicnumber*rhosteel*Csteel*(2*r3)^2/Ksteel,
      damping[imag,fibretype] ® (phisteel&),
      damping[imag,fibreatype] ® ((phisteel+deltafibre*(2*N[Pi]*#1*taufibre)
      /(1+(2*N[Pi]*#1*taufibre)^2))&),

      damping[imag,bladeUXtype] -> damping[imag,bladeUtype],
      damping[imag,bladeIXtype] -> damping[imag,bladeItype],
      damping[imag,bladeLXtype] -> damping[imag,bladeLtype]
};
```

6.2 Parameter set for monolithic build

```
overrides = {
      ribbons -> False,
      nx -> 0.1300, (* T040214-01 *)
      ny -> 0.5000, (* T040214-01 *)
      nz -> 0.0840, (* T040214-01 *)
      denn -> 4000, (* T040214-01 *)
      mn -> 21.924, (* BNS - measured 11/21/07 *)
      Inx -> 0.461468580178307, (* Model Fit: gradient_descent_fit_roll.m; BNS
            7/30/08 *)
      Iny -> 0.079141440690845, (* Model Fit: gradient_descent_fit_pitch.m; BNS
            7/30/08 *)
      Inz -> 0.46233, (* Model Fit: gradient_descent_fit_yaw.m; BNS 7/29/08 *)
      Inxy -> -0.033612681822167, (* Model Fit: gradient_descent_fit_roll.m;
            BNS 7/30/2008 *)
      Inyz -> 0.0000439, (* ? *)
      Inzx -> 0.00198, (* ? *)
      Inxz -> Inzx,
      Inzy -> Inyz,
```

```
Inyx -> Inxy,
ux -> 0.1300, (* T040214-01 *)
uy -> 0.5000, (* T040214-01 *)
uz -> 0.0840, (* T040214-01 *)
den1 -> 4000, (* T040214-01 *)
m1 -> 22.005, (* BNS - measured 11/21/07 *)
I1x -> 0.540861597136711, (* Model Fit: gradient_descent_fit_roll.m; BNS
      7/30/08 *)
I1y -> 0.077486282188856, (* Model Fit: gradient_descent_fit_pitch.m; BNS
      7/30/08 *)
I1z -> 0.51758, (* Model Fit: gradient_descent_fit_yaw.m; BNS 7/29/08 *)
I1xy -> -0.026034877679599, (* Model Fit: gradient_descent_fit_roll.m;
      BNS 7/30/08 *)
I1yz -> 0, (* ? *)
I1zx -> 0, (* ? *)
I1xz -> I1zx,
I1zy -> I1yz,
I1yx -> I1xy,
ix -> 0.1300, (* T040214-01 *)
ir -> 0.1570, (* T040214-01 *)
den2 -> 2200, (* not used *)
m2 -> 39.664, (* measured, BNS -  measured 11/21/07 *)
I2x -> 0.614736940669984, (* Model Fit: gradient_descent_fit_roll.m; BNS
      7/30/08 *)
I2y -> 0.407761183645900, (* Model Fit: gradient_descent_fit_pitch.m; BNS
      7/30/2008 *)
I2z -> 0.41557, (* Model Fit: gradient_descent_fit_yaw.m; BNS 7/29/08 *)
tx -> 0.1300, (* T040214-01 *)
tr -> 0.1570, (* T040214-01 *)
den3 -> 2200, (* not used *)
m3 -> 39.558, (* BNS -  measured 11/21/07 *)
I3x -> 0.614281054577945, (* Model Fit: gradient_descent_fit_roll.m; BNS
      7/30/08 *)
I3y -> 0.413139474164149, (* Model Fit: gradient_descent_fit_pitch.m; BNS
      7/30/08 *)
I3z -> 0.40046, (* Model Fit: gradient_descent_fit_yaw.m; BNS 7/29/2008
      *)
ln -> 0.448574, (* ? *)
l1 -> 0.308993, (* ? *)
l2 -> 0.341653, (* ? *)
l3 -> 0.600648, (* ? *)
rn -> (1.1/2)*10^-3, (* "Useful data for Noise Prototype Quad assembly";
      BNS 6/18/08 *)
r1 -> (0.71/2)*10^-3, (* "Useful data for Noise Prototype Quad assembly";
      BNS 6/18/08 *)
r2 -> (0.635/2)*10^-3, (* "Useful data for Noise Prototype Quad
      assembly"; BNS 6/18/08 *)
r3 -> If[ribbons, Indeterminate, Sqrt[0.00115*0.000115/Pi]],
t3 -> If[ribbons, 0.000115, Indeterminate], (* T060283 *)
W3 -> If[ribbons, 0.00115, Indeterminate], (* T060283 *)
optstress -> alphasilica*Ysilica/betasilica,
t3m -> t3,
W3m -> W3,
t3n -> Sqrt[m3*g/optstress/10/4],
W3n -> Sqrt[10*m3*g/optstress/4],
r3m -> r3,
r3n -> 0.000397494,
M31 -> If[ribbons, W3n t3n^3/12, Pi*r3n^4/4],
```

```
M32 -> If[ribbons, t3n W3n^3/12, Pi*r3n^4/4],
A3n -> If[ribbons, W3n t3n, Pi r3n^2],
A3m -> If[ribbons, W3m t3m, Pi r3m^2],
nf -> 1/40, (* neck fraction relative to total fibre -> about 1.5 cm or 5
      transverse flexure lengths *)
kw3 -> 1/(1/kw3m+2/kw3n), (* net longitudinal elasticity of fibres *)
kw3n -> Y3*A3n/(nf*l3), (* net longitudinal elasticity of one fibre neck
      *)
kw3m -> Y3*A3m/((1-2*nf)*l3), (* net longitudinal elasticity of fibre
      midsection *)
Yn -> 2.12000 10^+11, (* "As Designed Parameter Set 2"; BNS 6/18/08 *)
Y1 -> 2.12000 10^+11, (* "As Designed Parameter Set 2"; BNS 6/18/08 *)
Y2 -> 2.12000 10^+11, (* "As Designed Parameter Set 2"; BNS 6/18/08 *)
Y3 -> Ysilica, (* use same value as damping model (was independent in
      20061213TM) *)
kbuz -> 1411.4640262910420948351545480224, (* See matlab code
      spring_stiffness_calc: BNS 6/19/08 *)
kbiz -> 1650.5240590453796728792143217792, (* See matlab code
      spring_stiffness_calc: BNS 6/19/08 *)
kblz -> 2423.5190152802382310519860608100, (* See matlab code
      spring_stiffness_calc: BNS 6/19/08 *)
dm -> -0.003320022822893, (* Model Fit d's: gradient_descent_fit_pitch.m
      and gradient_descent_fit_roll.m; BNS 7/30/2008 *)
dn -> 0.002252503151706, (* Model Fit d's: gradient_descent_fit_pitch.m
      and gradient_descent_fit_roll.m; BNS 7/30/2008 *)
d0 -> -0.001663908530073, (* Model Fit d's: gradient_descent_fit_pitch.m
      and gradient_descent_fit_roll.m; BNS 7/30/2008 *)
d1 -> 0.002364277173936, (* Model Fit d's: gradient_descent_fit_pitch.m
      and gradient_descent_fit_roll.m; BNS 7/30/2008 *)
d2 -> 0.010-flex2,
d3 -> 0.001-flex3,
d4 -> 0.001-flex3,
sn -> 0,    (* T040214-01 *)
su -> 0.003,  (* T040214-01 *)
si -> 0.003,  (* T040214-01 *)
sl -> 0.015,  (* T040214-01 *)
nn0 -> 0.250,  (* T040214-01 *)
nn1 -> 0.090,  (* T040214-01 *)
n0 -> 0.200,  (* T040214-01 *)
n1 -> 0.060,  (* T040214-01 *)
n2 -> 0.140,  (* T040214-01 *)
n3 -> 0.1762, (* "As Designed Parameter Set 2"; BNS 6/18/08 *)
n4 -> 0.1712, (* "As Designed Parameter Set 2"; BNS 6/18/08 *)
n5 -> 0.1712, (* "As Designed Parameter Set 2"; BNS 6/18/08 *)
nwn -> 2,
nw1 -> 4,
nw2 -> 4,
nw3 -> 4,
mn3 -> mn+m13,
m13 -> m1+m23,
m23 -> m2+m3,
kbux -> 1.0 10^5,  (* as for middle *)
kbix -> 1.0 10^5,  (* Justin 11/29/05 *)
kblx -> 0.8 10^5,  (* Ian 12/09/05 *)
flexn -> Sqrt[nwn Mn1 Yn/(mn+m1+m2+m3)/g]*cn^(3/2),
flex1 -> Sqrt[nw1 M11 Y1/(m1+m2+m3)/g]*c1^(3/2),
flex2 -> Sqrt[nw2 M21 Y2/(m2+m3)/g]*c2^(3/2),
flex3 -> Sqrt[nw3 M31 Y3/m3/g]*c3^(3/2),
```

```
thetan -> 180 ArcSin[sin]/Pi,
theta1 -> 180 ArcSin[si1]/Pi,
theta2 -> 180 ArcSin[si2]/Pi,
theta3 -> 180 ArcSin[si3]/Pi,
DD -> Sqrt[M31 Y3/4/4/m3/g/sl3^2],

rhosilica -> 2.2 10^3, (* IFOModel v4.1 *)
Csilica -> 770., (* AH silica spec sheet, summary email by MB, 3/13/08 *)
Ksilica -> 1.38,  (* IFOModel v4.1 *)
sigmasilica -> 0.17,
Gsilica -> Ysilica/2/(1+sigmasilica), (* shear modulus *)
alphasilica -> 3.9 10^-7, (* AH measurement, summary email by MB, 3/13/08
      *)
betasilica -> 1.52 10^-4, (* IFOModel v4.1 *)
phisilica -> 4.1 10^-10, (* IFOModel v4.1 *)
phissilica -> 3. 10^-11, (* surface *)
Ysilica -> 7.2 10^10, (* AH spec sheet, summary email by MB, 3/13/08 *)
dssilica -> 1.5 10^-2, (* IFOModel v4.1 *)
sigmasilica -> 0.17,
Gsilica -> Ysilica/2/(1+sigmasilica), (* shear modulus *)

rhosteel -> 7800., (* gwinc/IFOModel v1.0 *)
Csteel -> 486., (* gwinc/IFOModel v1.0 *)
Ksteel -> 49., (* gwinc/IFOModel v1.0 *)
alphasteel -> 12. 10^-6, (* gwinc/IFOModel v1.0 *)
betasteel -> -2.5 10^-4, (* gwinc/IFOModel v1.0 *)
phisteel -> 2. 10^-4, (* gwinc/IFOModel v1.0 = Geppo's value  *)
Ysteel -> 2.12 10^+11, (* measured by MB, 11/18/05 *)

rhomarag -> 7800., (* gwinc/IFOModel v1.0 *)
Cmarag -> 460., (* gwinc/IFOModel v1.0 *)
Kmarag -> 20., (* gwinc/IFOModel v1.0 *)
alphamarag -> 11. 10^-6, (* gwinc/IFOModel v1.0 *)
betamarag -> -2.5 10^-4, (* Geppo's value - gwinc/IFOModel v1.0 is wrong
      *)
phimarag -> 1. 10^-4, (* gwinc/IFOModel v1.0 *)
Ymarag -> 1.87 10^11, (* gwinc/IFOModel v1.0 *)

(* Zener, 1938, Phys. Rev. 53:90-99 *)
magicnumber®1/4/FindRoot[0==D[BesselJ[1,x],x],{x,1.8}][[1,2]]^2,

tmU -> 0.0043, (* IFOModel v4.1 *)
deltabladeU ® Ymarag*alphamarag^2*temperature/(rhomarag*Cmarag),
taubladeU ® rhomarag*Cmarag*tmU^2/(Kmarag*N[Pi]^2),
damping[imag,bladeUtype] ® ((phimarag+
deltabladeU*(2*N[Pi]*#1*taubladeU)/(1+(2*N[Pi]*#1*taubladeU)^2))&),

tmI -> 0.0046, (* IFOModel v4.1 *)
deltabladeI ® Ymarag*alphamarag^2*temperature/(rhomarag*Cmarag),
taubladeI ® rhomarag*Cmarag*tmI^2/(Kmarag*N[Pi]^2),
damping[imag,bladeItype] ® ((phimarag+deltabladeI*(2*N[Pi]*#1*taubladeI)
/(1+(2*N[Pi]*#1*taubladeI)^2))&),

tmL -> 0.0042, (* IFOModel v4.1 *)
deltabladeL ® Ymarag*alphamarag^2*temperature/(rhomarag*Cmarag),
taubladeL ® rhomarag*Cmarag*tmL^2/(Kmarag*N[Pi]^2),
```

```
      damping[imag,bladeLtype] ® ((phimarag+deltabladeL*(2*N[Pi]*#1*taubladeL)
      /(1+(2*N[Pi]*#1*taubladeL)^2))&),

      deltawireU ® Ysteel*temperature
      *(alphasteel-betasteel*g*(mn+m1+m2+m3)/(nwn*N[Pi]*rn^2*Ysteel))^2
      /(rhosteel*Csteel),
      tauwireU ® magicnumber*rhosteel*Csteel*(2*rn)^2/Ksteel,
      damping[imag,wireUtype] ® (phisteel&),
      damping[imag,wireUatype] ® ((phisteel+deltawireU*(2*N[Pi]*#1*tauwireU)
      /(1+(2*N[Pi]*#1*tauwireU)^2))&),

      deltawireI ® Ysteel*temperature
      *(alphasteel-betasteel*g*(m1+m2+m3)/(nw1*N[Pi]*r1^2*Ysteel))^2
      /(rhosteel*Csteel),
      tauwireI ® magicnumber*rhosteel*Csteel*(2*r1)^2/Ksteel,
      damping[imag,wireItype] ® (phisteel&),
      damping[imag,wireIatype] ® ((phisteel+deltawireI*(2*N[Pi]*#1*tauwireI)
      /(1+(2*N[Pi]*#1*tauwireI)^2))&),

      deltawireL ® Ysteel*temperature
      *(alphasteel-betasteel*g*(m2+m3)/(nw2*N[Pi]*r2^2*Ysteel))^2
      /(rhosteel*Csteel),
      tauwireL ® magicnumber*rhosteel*Csteel*(2*r2)^2/Ksteel,
      damping[imag,wireLtype] ® (phisteel&),
      damping[imag,wireLatype] ® ((phisteel+deltawireL*(2*N[Pi]*#1*tauwireL)
      /(1+(2*N[Pi]*#1*tauwireL)^2))&),

      deltafibre ® Ysilica*temperature
      *(alphasilica-betasilica*g*(m3)/(nw3*A3n*Ysilica))^2
      /(rhosilica*Csilica),
      taufibre ® If[
      ribbons,
      rhosilica*Csilica*t3n^2/Ksilica/N[Pi]^2,
      magicnumber*rhosilica*Csilica*4*A3n/N[Pi]/Ksilica
      ],
      damping[imag,fibretype] ® If[
      ribbons,
      ((phisilica*(1+2*dssilica*(W3n+t3n)/(W3n*t3n)))&),
      ((phisilica*(1+2*dssilica/r3n))&)
      ],
      damping[imag,fibreatype] ® If[
      ribbons,
      ((phisilica*(1+2*dssilica*(3*nw3*W3n+t3n)*(W3n+t3n)/(nw3*W3n+t3n)/(W3n*t3
            n))
      +deltafibre*(2*N[Pi]*#1*taufibre)/(1+(2*N[Pi]*#1*taufibre)^2))&),
      ((phisilica*(1+4*dssilica/r3n)
      +deltafibre*(2*N[Pi]*#1*taufibre)/(1+(2*N[Pi]*#1*taufibre)^2))&)
      ],

      damping[imag,bladeUXtype] -> damping[imag,bladeUtype],
      damping[imag,bladeIXtype] -> damping[imag,bladeItype],
      damping[imag,bladeLXtype] -> damping[imag,bladeLtype]
};
```